Indonesian Journal of Electrical Engineering and Computer Science
Vol. 6, No. 2, May 2017, pp. 268 ~ 277
DOI: 10.11591/ijeecs.v6.i2.pp268-277

Symmetrical Short Circuit Parameter Differences of Double Fed Induction Generator and Synchronous Generator Based Wind Turbine

Muhammad Shahzad Nazir*[1], Qinghua Wu[2], Mengshi Li[3], Luliang Zhang[4]
[1,2,3,4]School of Electrical Power Engineering, South China University of Technology, Guangzhou, 510640, P.R. China
[2]Department of Electrical Engineering and Electronics, University of Liverpool, Liverpool L69 3GJ, U.K
*Corresponding author, e-mail: msn_bhutta88@yahoo.com[1], wuqh@scut.edu.cn[2]

Abstract

Considering the importance of perturbations during short circuit (SC) in power conversion devices, this study designed to find out the efficacy of symmetrical short circuit (SSC) of the synchronous generator (SG) and doubly fed induction generators (DFIG). Both wind power systems were separately built (Park's model) and simulated. Simulation results showed that the DFIG is more efficient, fault tolerant, and proficient systems as compared to the SG based on the transient time, steady state, maximum current, and voltage dip values. This study can extend to design protection schemes, more accurate, stable and optimal proficient wind power conversion devices.

Keywords*: Renewable energy, wind energy, doubly fed induction generator (DFIG), synchronous generator (SG), power system computer aided design (PSCAD)*

1. Introduction

Expansion of renewable power is the main strategy to meet the climate goals [1, 2]. The increase in power production from renewable energy sources would contribute 36% of wind power in 2035 [3]. Recently, the wind power production increased from 196.63GW to 240GW [4]. Wind energy can be converted into electrical energy by different types of energy converters. The wind energy conversion system (WECS) has two main types, the DFIG, and the SG. The DFIG is an economical, variable speed, light weight and easy to control power conversion system [5-8]. The DFIGs are also known as the doubly fed asynchronous generator. The DFIGs are variable speed generators, having merits as compared to the other electricity generation systems [9-12]. They are widely used in wind turbine applications due to high-energy efficiency and improved power quality [7], [13, 14]. The DFIG-based wind generator system consists of six parts: the wind turbine system (mechanical part), the DFIG generator, the rotor side converter (RSC), the DC link, the grid side converter (GSC and its filter) and the control system. The electronic converters in DFIGs are connected to the stator (part of a rotary system to keep the field aligned) winding linked with the three-phase load/grid, while the rotor side windings connected to a back to back power converter [15].

The othertype of WECS called synchronous generator (SG). SG is called "synchronous" because the waveform of the generated voltage is synchronized with the rotation of the rotor speed. In SG, the magnetic field of the rotor is supplied by the separate direct current (DC) or permanent magnets for excitation. The advantage of SG is the use of the comparatively small size of converters [6], [16]. Both generators (DFIG & SG) are under consideration for major types of electric power generation industries. According to the recent review of state of the art has been noticed that highly leaning DFIG and SG for wind power on the large and small scale, respectively [6].

The selection of wind power systems can play a significant role in the total amount of power generations. Therefore a comparison of different power conversion systems becomes important. The perturbation conditions (short-circuit, voltage-dip, steady state, transient time etc.) study can help to improve the resilience of wind power systems. That can also minimize the power losses. We used simulation analysis of both wind power generators (DIFG and SG) to

Received January 2, 2017; Revised March 14, 2017; Accepted April 1, 2017

understand merits, demerits and identify the power losses. This study presents a highly desirable comparison of DIFG and the SG based on the short circuit (three-phase or symmetrical).

Our study also describes the transient time value difference of the short circuit current in both generators (DIFG and SG), such as, manifested steady state, maximum current, and voltage dip values. Both systems were simulated in PSCAD/EMTDC platform with different points and SC fault resistance values. Three-phase SC fault results were obtained asin the form of graphs and explained by the Tables along with related equations. Overall, this paper is organized in following sections. Section 2 and 3 illustrates the simulation and mathematical model of both wind systems. Then section 4 manifests the simulation results. Discussion summarized in section 5. Conclusions are given in section 6.

2. Simulation Model of DFIG And SG

Two wind power systems (DFIG and SG) separately built by the editing in PSCAD/EMTDC library according to the requirement for better understand the behaviors of two systems under fault conditions (symmetrical or three-phase). Figure 1a and 1b; schematically represent the generator systems, where K_1 and K_2 represent the fault points. The appendix shows different parameters, the ratings of DFIG and SG were kept the same for better comparison.

2.1. Wind Power Versus Generator Characteristics

Wind energy can be converted into mechanical energy (wind turbine), which later transforms into electrical energy [17]. Generators of wind turbines require following general characteristics:

1. Reduction of the system components
2. High torque and power density
3. Better efficiency and cost effectiveness
4. High reliability and robustness under different wind operating conditions
5. Comparatively easier maintenance than other power generator systems

Moreover, electrical generators should be tolerant under fault conditions and extreme environment. The power response at different wind speeds is the main factor affecting the efficiency of wind turbines [16, 17].

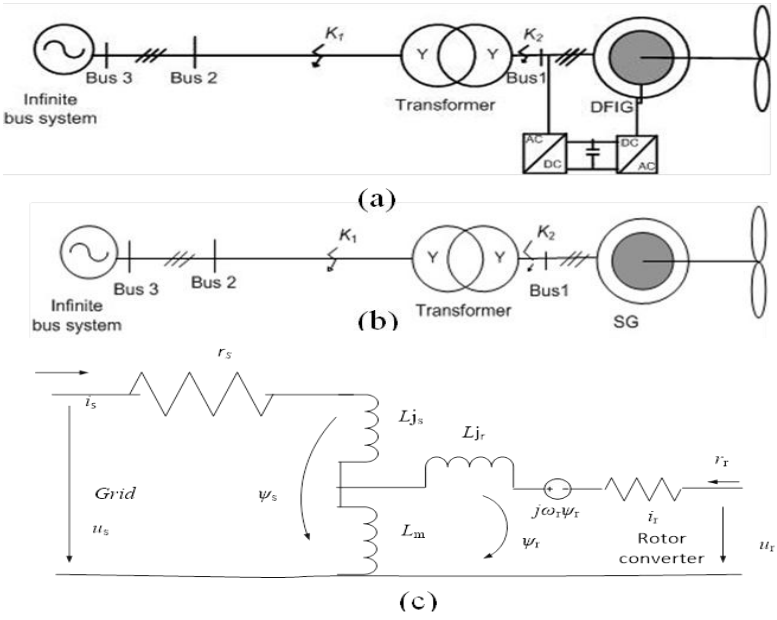

Figure 1. Wind park system with equivalent circuit
(a) DFIG-WT system, (b) SG-WT system, (c) Equivalent circuit of Park's model

2.2. Wind Power Conversion Method

The first motive of wind system is strong and sufficient wind speed (v_w) at wind farm sectors. The wind power law has been identified [1], [18].The aerodynamics power (P_t) is given by the betz, refer to (1).

$$P_t = \frac{1}{2}\rho S v_w^3 C_p(\lambda) \tag{1}$$

Whereρ = air density (kg/m3), S = surface area of the turbine blade (m^2), v_w = wind speed (m/s), and $C_p(\lambda)$ = aerodynamic conversion factor. The *Cp* is a function of lambda (λ, tip speed ratio), refer to (2) which relates to the wind speed with rotor speed.

$$\lambda = W\frac{R}{v_w} \tag{2}$$

Where *R* is the blade radius (m), *W* is the rotational rotor speed (rad/s). The torque produced (*T*, by the wind-speed v_w) at the rotor of turbine refer to (3).

$$T = kv_w^2 \tag{3}$$

A direct drive (DD) power generator rotates at the same speed as the turbine, therefore there is same torque.

3. Mathematical Model

For simulation, invoking the matrix C3s→2r, the voltage and magnetic flux under *d-q* reference frame [19-21] can be expressed by the following stator and rotor voltage refer to (4 and 5, zero sequence is neglected),

$$\begin{cases} u_{ds} = r_s i_{ds} - \omega\psi_{qs} + \dfrac{d}{dt}\psi_{ds} \\ u_{qs} = r_s i_{qs} - \omega\psi_{ds} + \dfrac{d}{dt}\psi_{qs} \end{cases} \tag{4}$$

$$\begin{cases} u_{dr} = r_s i_{dr} - (\omega_1 - \omega_r)\psi_{qr} + \dfrac{d}{dt}\psi_{dr} \\ u_{qr} = r_s i_{qr} + (\omega_1 - \omega_r)\psi_{dr} + \dfrac{d}{dt}\psi_{qr} \end{cases} \tag{5}$$

Where,$\omega_1 - \omega_r = \frac{d(\varphi - \theta_r)}{dt}$, the magnetic flux ($\psi$) related with the referring to (6 and 7) under *d-q* reference, and stator and rotor voltage (u_s and u_r) refer to (8 and 9):

$$\begin{cases} \psi_{ds} = L_s i_{ds} + L_m i_{dr} \\ \psi_{qs} = L_s i_{qs} + L_m i_{qr} \end{cases} \tag{6}$$

$$\begin{cases} \psi_{dr} = L_r i_{dr} + L_m i_{ds} \\ \psi_{qr} = L_r i_{qr} + L_m i_{qs} \end{cases} \tag{7}$$

$$u_s = r_s i_s + \frac{d}{dt}\psi_s \quad (8)$$

$$u_r = r_r i_r + \frac{d}{dt}\psi_r - j\omega_r \psi_r \quad (9)$$

We first composed d and q components then referred the rotor variables to the stator by the Park's model [20]. Here, it can be expressed as the stator and rotor flux (ψ_r&ψ_s) and voltage (u_r) are referred to (10, 11, 12 and 13).

$$\psi_s = L_s.i_s + L_m i_r \quad (10)$$

$$\psi_r = L_r.i_r + L_m i_s \quad (11)$$

$$\psi_r = \frac{L_m}{L_s}\psi_s - \sigma L_r i_r \quad (12)$$

$$u_r = \frac{L_m}{L_s}(\frac{d}{dt} - j\omega_r)\psi_s + (r_r + \sigma L_r(\frac{d}{dt} - j\omega_r))i_r \quad (13)$$

Where u_r, u_s, ψ_r, $\psi_s i_r$, i_s are the voltage, current, and flux in the stator and rotor; r_s, r_r, L_s, L_r,are the stator and rotor, resistance, inductance, L_m is the mutual inductance of the generator; ω_r is the electrical angular velocity of the rotor and the leakage factor denoted as $\sigma = (1 - L_m^2/L_s L_r$.

The Figure 1c shows the equivalent circuit according to the Park's model [20, 21]. The model extends to the rotor flux variation expressed refer to (11 and 12). We substitute by (12 into 9), and obtained (13), which corresponds to the rotor voltage.

Equation (13), can be divided into two terms; the first, u_{ro} due to stator flux, or forced component. When the rotor assumes an open-circuit condition (i_r = 0), it is called rotor current. This term only appears when current flows into the rotor, which is also known as a natural component. When the power system failure occurs then this term will suffer drastic change due to the voltage drop in both the rotor resistance and transient inductance (σL_r). It contributes toward natural component of rotor current (i_r).

4. Simulation Results

4.1. Three-Phase Short Circuit at Low and High Voltage Side

4.1.1. The Symmetrical Short Circuit at High Voltage Side

Firstly, short circuit behavior was observed in DFIG at the high voltage side. To achieve this condition, we applied the short circuit after the transformer. A three-phase short circuit (Symmetrical) fault was applied at 1.5 s for 1 s while the SC fault applied resistance value was 0.035 Ω. The resulting value of maximum three-phase SC current was 5.1 p.u. As the time elapsed, the current decayed exponentially based on the time constant, determined by the fault resistance, impedance of DFIG and transformer components. The decay ends after about 0.51 s. Current decayed completely to its minimum value at 1.83 s (Figure 2a). The SC was applied between the bus 2 and the transformer, then the observed values Figure 2a, are summarized in the Table 1. Once again, the system was short-circuited for 1 s starting from 1.5 s. The short circuit resistance value was 0.035 Ω. Maximum three-phase short circuit current increased towards 12.80 p.u and current decayed exponentially based on the time constant (τ). The decay ends after 0.65 s and the steady state current is 4.74 p.u. When similar conditions were applied on the SG system, the observed SC values (Figure 2b) are summarized in Table 1.

We further studied voltage behavior (high voltage side) for the DFIG and SG system. The simulation results indicated the voltage dip values. For the DFIG system, firstly the voltage

shows fluctuation from 0.6 p.u to 0.1 p.u for about 0.28 s. After employing the short circuit, it decreased towards its minimum value, whereas voltages dip directly towards the minimum value in the SG system, Figure 2c, 2d respectively.

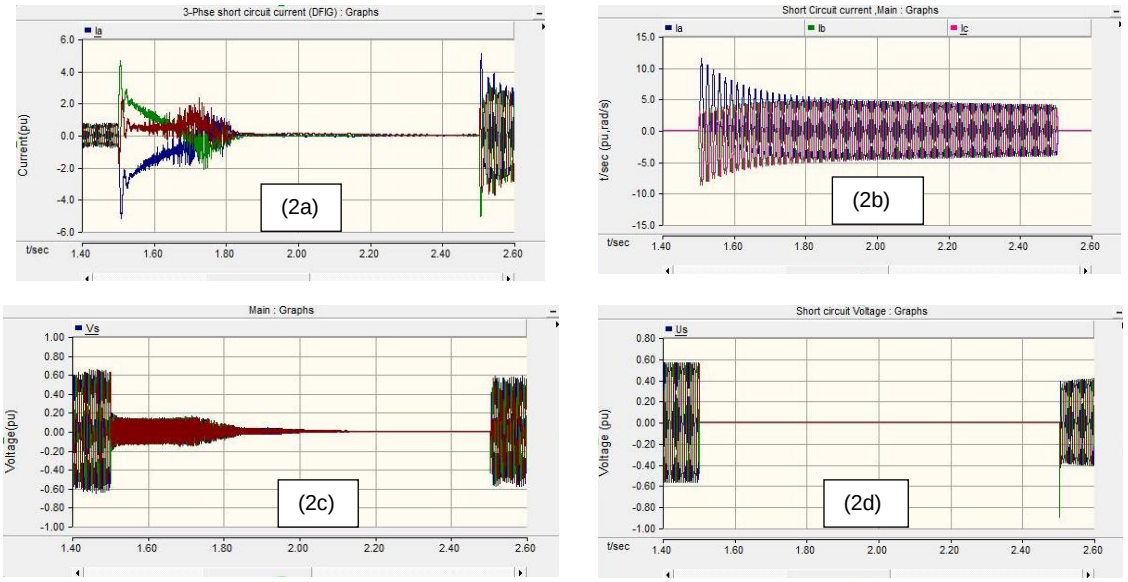

Figure 2. Symmetrical short circuit current and voltage at HV side
(a) Short circuit current of DFIG, (b) Short circuit current of SG, (c) Short circuit voltage of DFIG, (d) Short circuit voltage of DFIG

4.1.2. The Symmetrical Short Circuit at Low Voltage Side

We compared both generators by considering the short circuit (SC) at low voltage side after the generator (before transformer). The Figure 3a depicts the SC transient behavior of the DFIG system at low voltage. The transient process begins at 1.50 s and ends at 1.52 s; simulation results showed 0.02 s transient value. This time duration of the transient is smaller (0.02 s). When a fault occurs at high voltage side the impedance was smaller, so the maximum current is larger (5.1 p.u). Hence, it realizes that steady state value of the SSC is about 1 p.u after 1.52 s. The fault point affects the value of the time constant (τ).The time constants referred to in this standard are only valid for three-phase fault currents. The parameters of the DFIG indicate$\tau_h < \tau_l$. The Figure 3b depicts the SC transient behavior of the SG system at low voltage side. The transient process begins at 1.50 s and ends at 1.53 s, implying that the transient time is 0.03 s. This time duration of the transient is small (0.03 s). The parameters of the DFIG indicate that$\tau_h < \tau_l$.

When a fault occurs at the high-voltage side the impedance was smaller, so the maximum current is larger (8 p.u). Hence, it realizes that steady state value of SSC is about 3.9 p.u after 1.53 s. The fault (SC) depicts maximum current = 12.80 p.u (Figure 2b) at the high-voltage side. The Figure 3c depicts the behavior of voltage at the low voltage (LV) side of the DFIG system. The voltage fluctuates to its half value and once SC was employed, it fluctuates from 0.60 p.u to 0.33 p.u (Table 1). The Figure 3d depicts voltage fluctuations are approximately three times of the total value once the short circuit is employed. The transient time results indicate the different change for the DFIG on both sides when compared with the SG system.

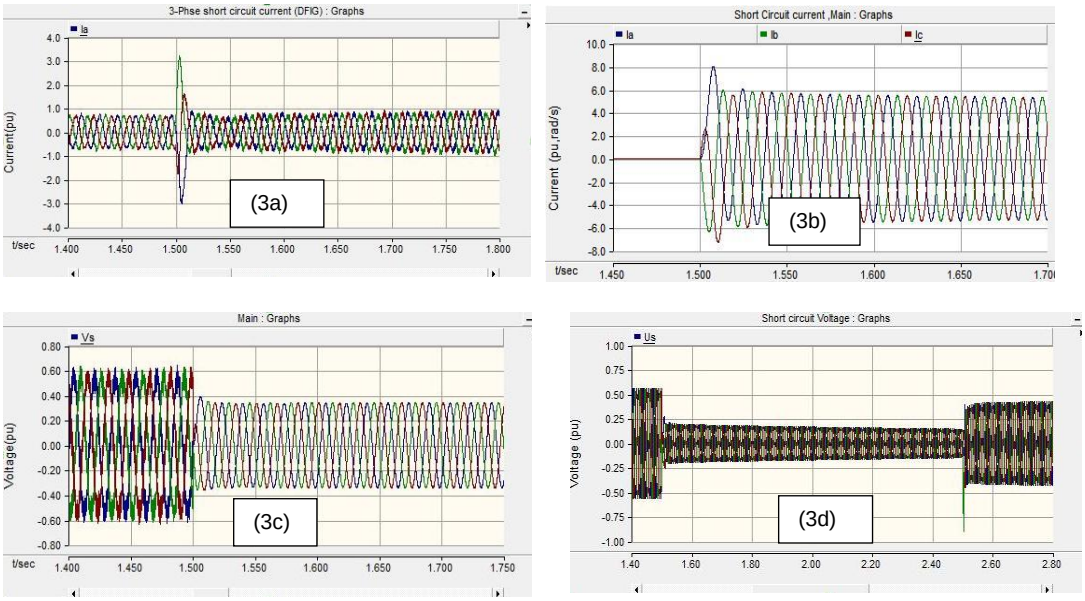

Figure 3. Symmetrical short circuit current transient process and voltage fluctuation at LV side (a) Transient process of DFIG, (b) Transient process of SG, (c) Voltage fluctuation of DFIG, (d) Voltage fluctuations of SG

4.2. Three-Phase Short Circuit at Transmission Line

In this section, we present the third point of SC fault (Table 1) at the midpoint of the transmission line (TL). The both systems (DFIG and SG) parameter values were kept same (Table 2 and 3). The SC was applied at the TL during 1.5 s continued for 1 s. The Figure 4a shows the SC transient time resulting simulation of the DFIG system, which depicts that the transient time of SC in the DFIG system was 0.28 s. The SC steady state value of the DFIG system is 0.61 p.u and the maximum current value was 4 p.u. The equivalent of transmission line resistance is 0.4 Ω and the value of inductance was 1.25 H.

The transient time difference in both systems is about 0.05 p.u (Figure 5c, 5d and Table 1). The SG shows three times maximum SC current than the DFIG. The Figure 4c depicts voltage behavior in DFIG system and Figure 4d voltage behavior of SG. There voltage fluctuates between 0.55 p.u-0.02 p.u for the DFIG and 0.55 p.u-0.04 p.u for the SG (Table 1, Figure 4c and 4d). The maximum current value for DFIG and SG is 4p.u and 11.40p.u (Table 1), respectively. This value is three times higher than DFIG.

Table 1. Numerical values of low, high voltage sides and transmission line

Generator/ Transmission line	Transient time (s)	Maximum current(p.u)	Steady state current(p.u)	Voltage dip (p.u)
DFIG(H*)	0.33	5.1	0.30	0.6-0.18
SG(H*)	0.65	12.80	4.74	0.6-0.12
DFIG(L*)	0.02	3.1	1	0.6-0.33
SG(L*)	0.03	8	3.9	0.6-0.18
DFIG(TL*)	0.26	4	1.2	0.55-0.02
SG(TL*)	0.31	11.40	5	0.55-0.04

The *H, L* and TL* denote the high, low voltage sides and transmission line, respectively.

We observed the transient time and maximum current value of both generators (Table 1). According to the simulation results, the DFIG depicts more effective response during the SC. The DFIG system shows lower maximum current value than the SG which shows lesser sensitivity during three-phase SC because the SG system has about twice the value of maximum current as compared to the DFIG system. Hence, simulation results are illustrating the robustness of the DFIG system. Another prominent factor is that the time employed for the

fault of both generators is equal but the transient time of both generators is observed different (Table 1, Figure 3b). The SG system needs more time (Figure 3a, 3b and Table 1) at LV side than DFIG to resist the SC. These observations conclude that at high voltage side, the DFIG shows more effective behavior than the SG according to the transient time, maximum current and steady state value respectively.

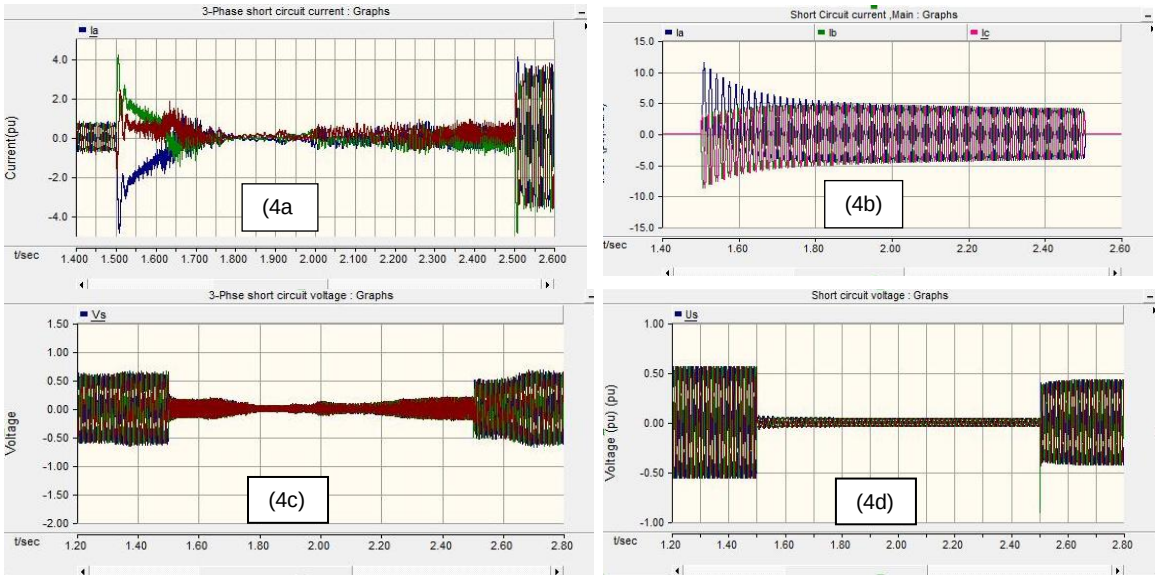

Figure 4. Symmetrical short circuit current and voltage at midpoint of TL
(a) Short circuit current of DFIG, (b) Short circuit current of SG, (c) Short circuit voltage of DFIG, (d) Short circuit voltage of SG

5. Discussion

5.1. Basic Operational Differences

The main difference between these two generators is the process of excitation current. The SG generates an exciting current through its rotor. However, DFIG needs an external source of exciting current that stimulate it to generate current in both rotor and stator. The stator side converter generates stator exciting current, as DFIG has crowbar protection; the system under fault condition that isolates rotor from the system which makes DFIG depends on the stator current. A crowbar circuit operates by putting a short circuit or low resistance path across the voltage output (V_o). In active crowbar system, DFIG acts like traditional induction generator (IG). When crowbar is not in operation then rotor of DFIG can also generate the current by rotor side converter. A detailed discussion on both systems is given in the following sections.

5.2. Amplitude Comparison

Current amplitude (I_0 or I_1) is the measurement of the degree of positive or negative change in current (K). In this section, SC has been applied at high voltage side of DFIG and SG, respectively. It was employed at the 1.5 s up to 1 s, while the applied fault resistance kept at 0.035 Ω, according to the simulation results of the DFIG and SG system (Figure 5a and 5b), respectively. Where I_{0DFIG} is 4.46 p.u and I_{1DFIG} is 2.06 p.u. So, if we put these values in (14).

$$K_{DFIG} = I_{0DFIG} - I_{1DFIG} \quad (14)$$

Here $I_{0DFIG}$is the peak (maximum) value of current and I_{1DFIG} is its minimum value, K is the resulting value between the I_{1DFIG} and I_{0DFIG}. After assigning the value of $I_{1DFIG}$and I_{0DFIG} in (14), we obtained K_{DFIG}.

$$K_{DFIG} = 4.46 - 2.06 = 2.40 \text{ p.u} \quad (15)$$

We observed (Figure 5b) the SCC amplitude value ofK_{SG}, I_{1SG} andI_{0SG}. The $I_{0SG}$is 12.68 p.u and $I_{1SG}$is 5 p.u. Therefore referring to (16).

$$K_{SG} = I_{0SG} - I_{1SG} \quad (16)$$

$$K_{SG} = 12.98 - 5 = 7.98 \text{ p.u} \quad (17)$$

The comparison of $K_{SG}$and K_{DFIG}, referring to (15 and 17), which shows that K_{SG}> K_{DFIG}. The amplitude value of $K_{SG}$is about three times larger than K_{DFIG}.

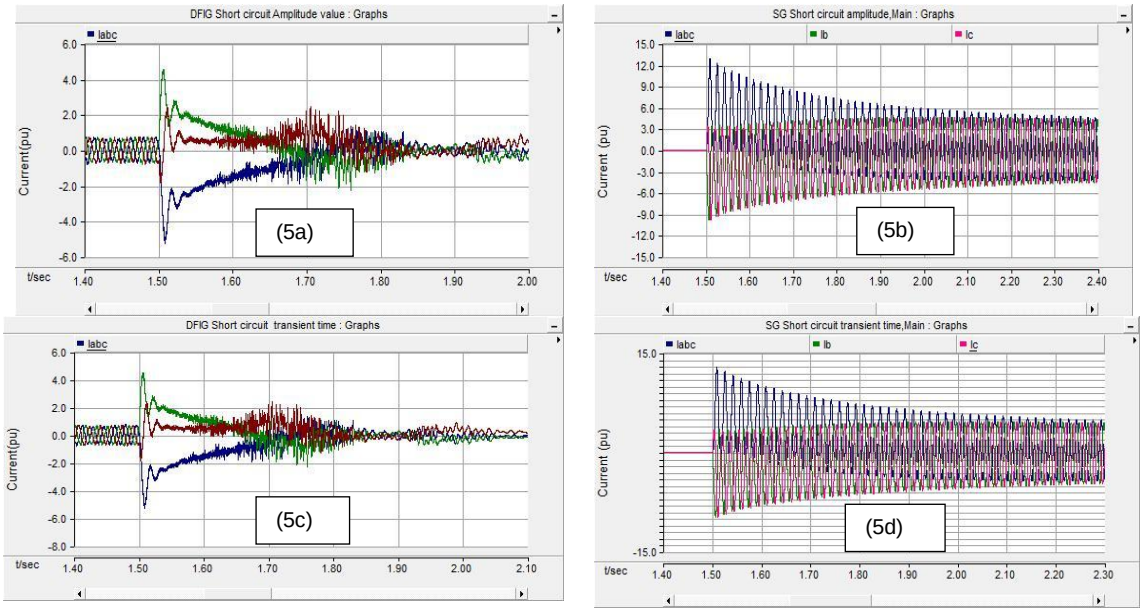

Figure 5. Short circuit current amplitude and transient time of DFIG and SG
(a) DFIG short circuit current amplitude, (b) SG short circuit current amplitude,
(c) Short circuit transient time value of DFIG, (d) Short circuit transient time value of SG

5.3. Transient Time Difference

The time required for the transient or natural response of a system to a change from equilibrium or a steady state is known as transient time. The SC applied at high voltage side at time 1.5 s for applied fault duration of 1 s with SC resistance 0.035 Ω. The Figure 5c and 5d depict the transient value of the two systems, respectively. The Figure 5d also depicts that after the fault occurrence, the decay of the current lasts for about 0.5 s in SG, which is a longer time when compared to the DFIG systemand where this duration is about 0.32 s. Transient process is longer which indicates that total resistance is smaller.

5.4. Steady-State Value Difference

After the transient state, the current approaches its steady value, then it is known as steady state current. The SC occurs at high voltage side for 1.5 s kept for 1 s, with fault resistance = 0.035 Ω. The Figure 6a depicts the steady state current value of DFIG. After short circuit occurs, the fault value of steady state current found 1.2 p.u. The Figure 6b shows that the SG has 5 p.u, steady state current. This value is larger than DFIG's steady state current value.

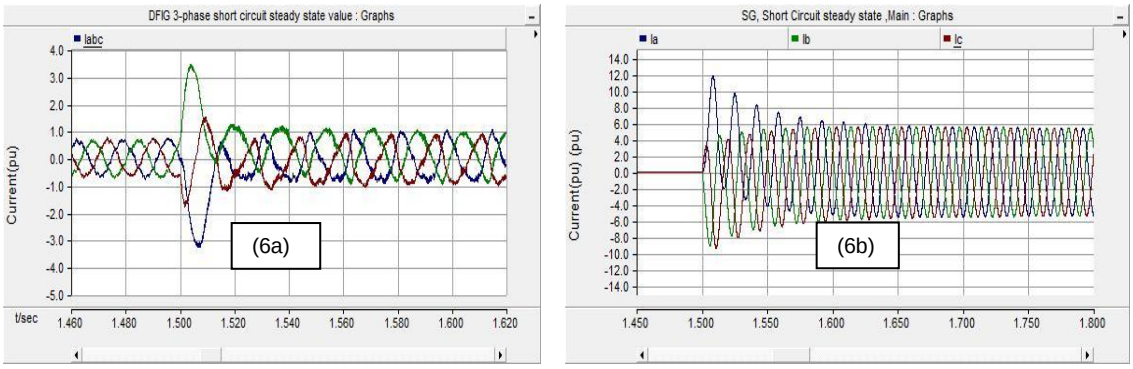

Figure 6. Steady state value of DFIG and SG: (a) DFIG value, (b) SG value

6. Conclusion

In this research, we have comparedtwo types of wind power applications. The comparative simulation study of short circuits of different parameters differences of DFIG and SG proves that the DFIG is a better option for the power generation. Short circuit was applied in the DFIG and SG systems. We compared the respective SC values by simulation. Results indicate that at 0.035 Ω, DFIG provides shorter transient time and maximum current value than the SG at HV side. The DFIG (LV side) with same SC resistance value also displays shorter transient time and about three times lower maximum current. A three-phase SC fault was also applied at the midpoint of TL. When the DFIG and SG systems were short-circuited, the DFIG transient time, steady state values and voltage fluctuation values were two and three times lower than the SG. This study supports to improve the perturbations, protection schemes, design more accurate, stable and optimal proficient WECS.Following these results will help to build a proficient control, protection schemesfor perturbation conditons (short circuit faults) of WECS based on DFIG.

Acknowledgement

This research is supported by the State Key Program of National Natural Science Foundation of China (No. 51437006) and Guangdong Innovative Research Team Program (No. 201001N0104744201), China. Mr. Muhammad Shahzad Nazir highly appreciate Chinese Scholarship Council (CSC) and School of Electrical Power Engineering, South China University of Technology (SCUT).

References

[1] Lebsir A, Bentounsi A, Benbouzid M, Mangel H. Electric generators fitted to wind turbine systems: An up-to-date comparative study. *Journal of Electrical Systems*. 2015; 11(3): 281–295.
[2] Wang L, Truong D N. Stability enhancement of a power system with a PMSG-based and a DFIG-based offshore wind farm using a SVC with an adaptive-network-based fuzzy inference system. *IEEE transactions on industrial electronics*. 2013; 60(7): 2799-2807.
[3] Ezzaidi A, Elyaqouti M, Bouhouch L, Ihlal A. Evaluation of the Energy Performance of the Amougdoul Wind Farm, Morocco. *International Journal of Electrical and Computer Engineering (IJECE)*. 2017; 7(2).
[4] Khater F, Omar A. A review of direct driven pmsg for wind energy systems. *Journal of Energy and Power Engineering*. 2013; 7(8).
[5] Cherfia N, Kerdoun D. Wind Energy Conversion Systems Based On a DFIG Controlled By Indirect Vector Using PWM and SVM. *International Journal of Electrical and Computer Engineering (IJECE)*. 2016; 6(2): 549.
[6] Yousefian R, Bhattarai R, Kamalasdan S. Transient Stability Enhancement of Power Grid with Integrated Wide-Area Control of Wind Farms and Synchronous Generators. *IEEE Transactions on Power Systems*. 2017.
[7] Elfaki O, Zezhong W, Qihui L. Behavior of DFIG wind turbine during unbalanced grid voltage. *Indonesian Journal of Electrical Engineering and Computer Science*. 2014; 12(7): 4934-4943.

[8] Hughes FM, Anaya-Lara O, Jenkins N, Strbac G. Control of DFIG-based wind generation for power network support. *IEEE Transactions on Power Systems*. 2005; 20(4): 1958-1966.
[9] Ayodele TR, Ogunjuyigbe ASO. Wind energy resource, wind energy conversion system modelling and integration: a survey. *International Journal of Sustainable Energy*. 2015; 34(10): 657-671.
[10] Elbashir OE, Zezhong W, Qihui L. Analysis of DFIG Wind Turbine During Steady-State and Transient Operation. *TELKOMNIKA Indonesian Journal of Electrical Engineering*. 2014; 12: 4148-4156.
[11] Swain S, Ray PK. Short circuit fault analysis in a grid connected DFIG based wind energy system with active crowbar protection circuit for ridethrough capability and power quality improvement. *International Journal of Electrical Power & Energy Systems*. 2017; 84: 64-75.
[12] Civelek Z, Çam E, Lüy M, Mamur H. Proportional–integral–derivative parameter optimisation of blade pitch controller in wind turbines by a new intelligent genetic algorithm. *IET Renewable Power Generation*. 2016; 10(8): 1220-1228.
[13] Muller S, Deicke M, De Doncker RW. Doubly fed induction generator systems for wind turbines. *IEEE Industry applications magazine*. 2002; 8(3): 26-33.
[14] Liu Y, Wu QH, Zhou XX, Zhou L. Perturbation observer based multiloop control for the DFIG-WT in multimachine power system. *IEEE Transactions on Power Systems*. 2014; 29(6): 2905-2915.
[15] Li H, Chen Z. Overview of different wind generator systems and their comparisons. *IET Renewable Power Generation*. 2008; 2(2): 123-138.
[16] Sridharan S, Manonmani N. Modeling and Simulation of Grid Interfaced Synchronous Generator with Controller. *Indonesian Journal of Electrical Engineering and Computer Science*. 2014; 12(12): 8098-8103.
[17] Kaldellis JK, Zafirakis D. The wind energy (r) evolution: A short review of a long history. *Renewable Energy*. 2011; 36(7): 1887-1901.
[18] Rosli MA, Yahaya NZ, Baharudin Z. Multi-input DC-AC Inverter for Hybrid Renewable Energy Power System. *International Journal of Electrical and Computer Engineering (IJECE)*. 2016; 6(1): 40.
[19] Kothari DP, Nagrath IJ. Modern power system analysis. Tata McGraw-Hill Education. 2003.
[20] Park RH. Two-reaction theory of synchronous machines generalized method of analysis-part I. *Transactions of the American Institute of Electrical Engineers*. 1929; 48(3): 716-727.
[21] Morren J, De Haan SWH. Short-circuit current of wind turbines with doubly fed induction generator. *IEEE Transactions on Energy conversion.* 2007; 22(1): 174-180.

Appendix

Wind Park

Table 2. Parameters of DFIG

Parameters	Value (p.u)	Parameters	Value (p.u)
R_s (resistance)	0.0054	L_s (leakage inductance)	0.10
L_m (mutual inductance)	4.5	R_r (resistance)	0.0060
L_r (leakage inductance)	0.11	Mechanical damping	0.0001
Rated power	0.9 [MVA]	Frequency	50 [Hz]

pu = per unit ; l-l= line to line

Table 3. Parameters of SG

Parameters	Value (p.u)
Rated rms *l-l* natural voltage	0.398
Rated RMS line current	1.306